

A biocompatible NIR-II light-responsive nanoknife for permanent male sterilization

Haoyu Wang,^{a,b,‡} Xiaomeng Yue,^{c,‡} Huanhuan Wu,^a Yeda Wan,^c Yujie Tong,^a Yang Zhao,^d Yijun Li,^e and

Jinbin Pan^{a,}*

- a. Department of Radiology, Tianjin Key Laboratory of Functional Imaging, Tianjin Medical University General Hospital, Tianjin 300052, China.
- b. Department of Radiology, Affiliated Hospital of Inner Mongolia Medical University, Hohhot 010050, China.
- c. Ultrasonic Diagnosis and Treatment Department, National Clinical Research Center of Cancer, Tianjin Cancer Hospital Aripport Hospital, Tianjin 300052, China.
- d. Department of Radiology, The Second Hospital of Tianjin Medical University, Tianjin 300211, China.
- e. Inner Mongolia Medical University, Hohhot 010050, China.

‡ These authors contributed equally to this article.

*Corresponding authors. E-mail:panjinbin@tmu.edu.cn

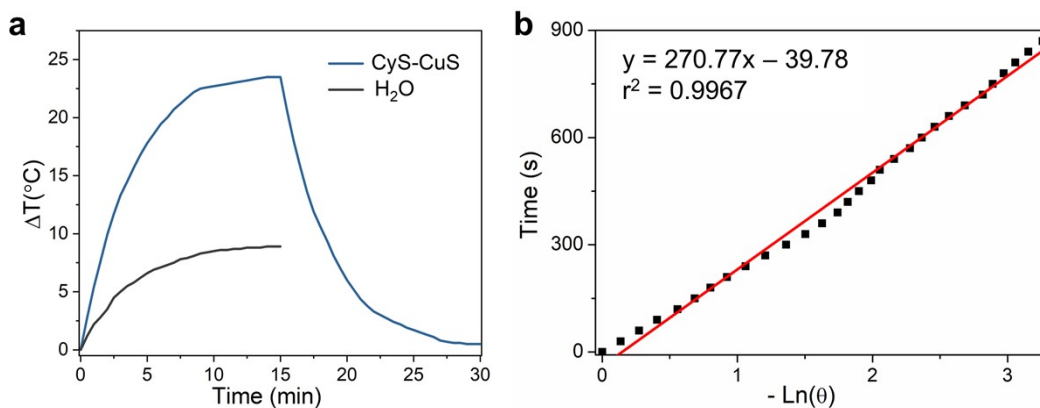


Figure S1. Temperature evolution curves of Cys-CuS nanosheets in a 1064 nm laser on/off cycle. a) Temperature profile of Cys-CuS solution (100 mg L^{-1}) under the irradiation of a 1064 nm laser (2.0 W cm^{-2}) for 15 min, and then the laser was turned off. b) Plot of the cooling time versus $-\ln(\theta)$ obtained from the cooling stage in (a).

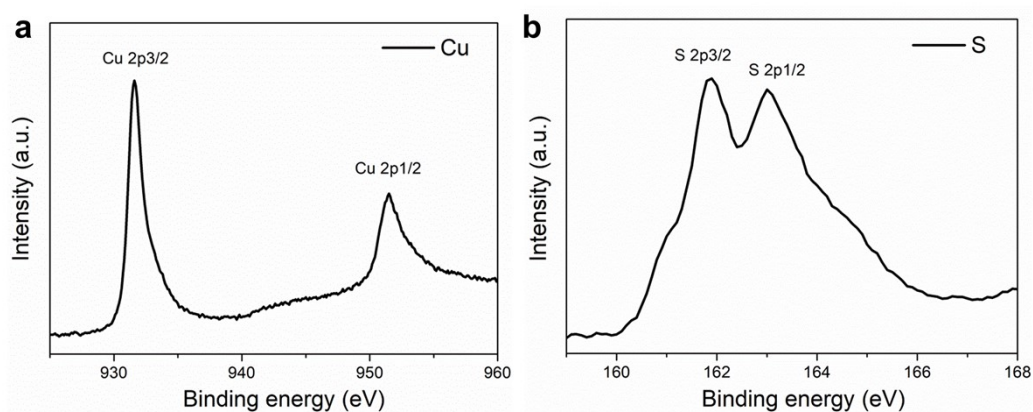


Figure S2. XPS spectra of (a) Cu 2p and (b) S 2p in Cys-CuS nanosheets.

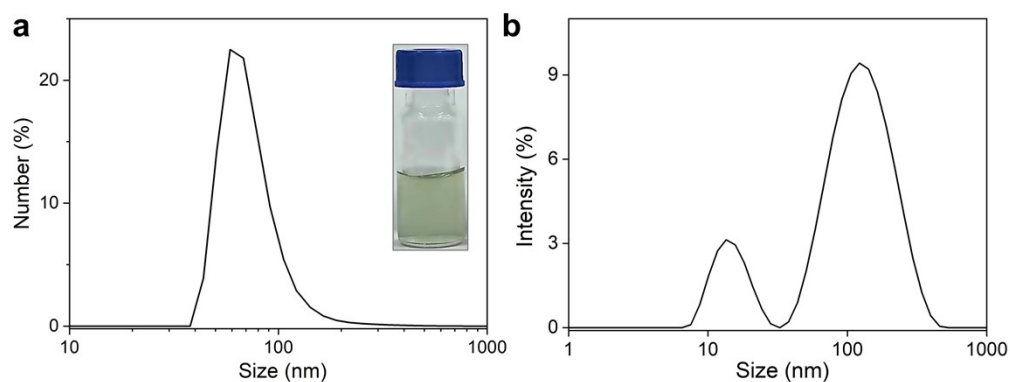


Figure S3. Hydrodynamic size of Cys-CuS nanosheets measured by DLS. The insert photograph is Cys-CuS aqueous solution (0.04 mg mL^{-1}).

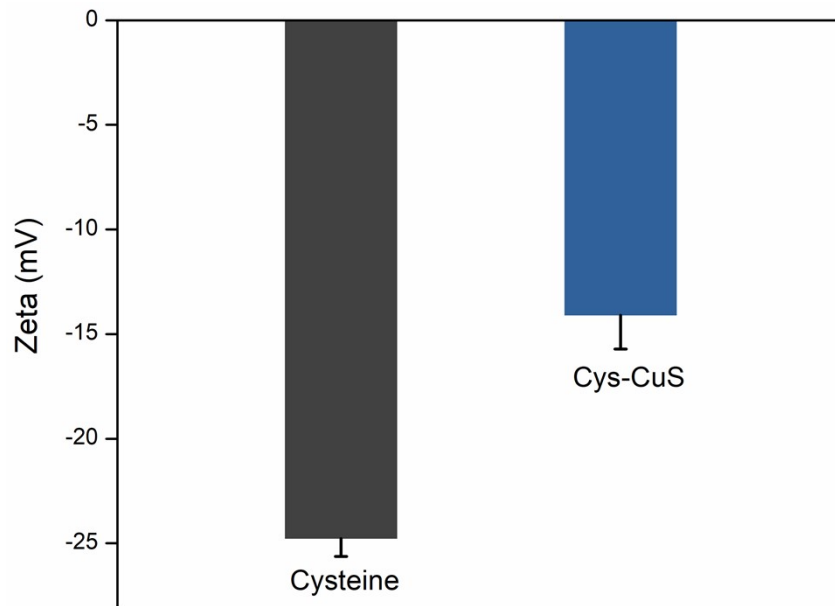


Figure S4. The zeta potential of Cystine and Cys-CuS nanosheets.

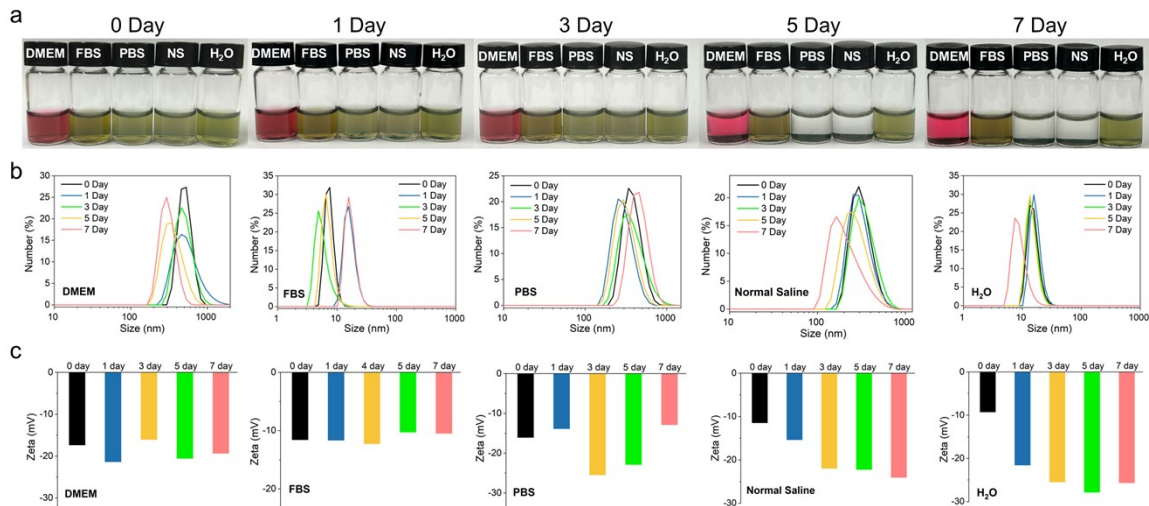


Figure S5. The photograph (a), DLS (b) and zeta potential (c) of Cys-CuS in PBS, normal saline, DMEM, fetal bovine serum (FBS), and deionized water at different time points (0, 1, 3, 5, 7 days)

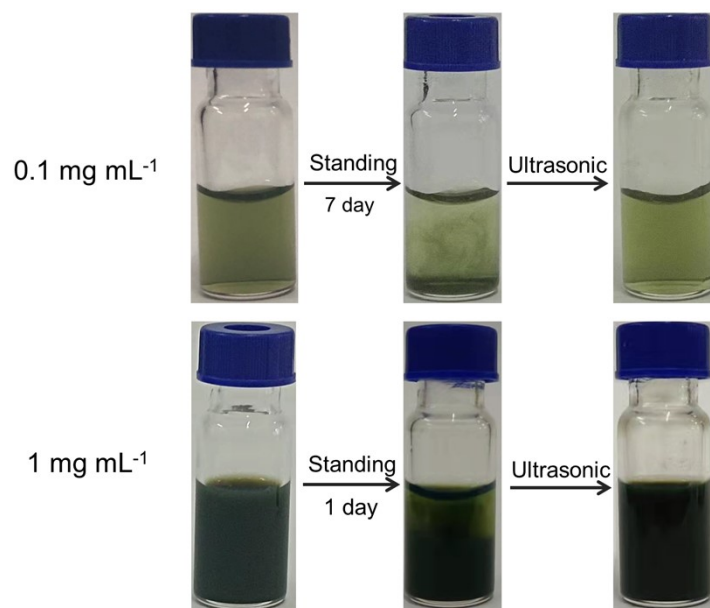


Figure S6. Photographs of Cys-CuS nanosheets solutions after standing for some time.

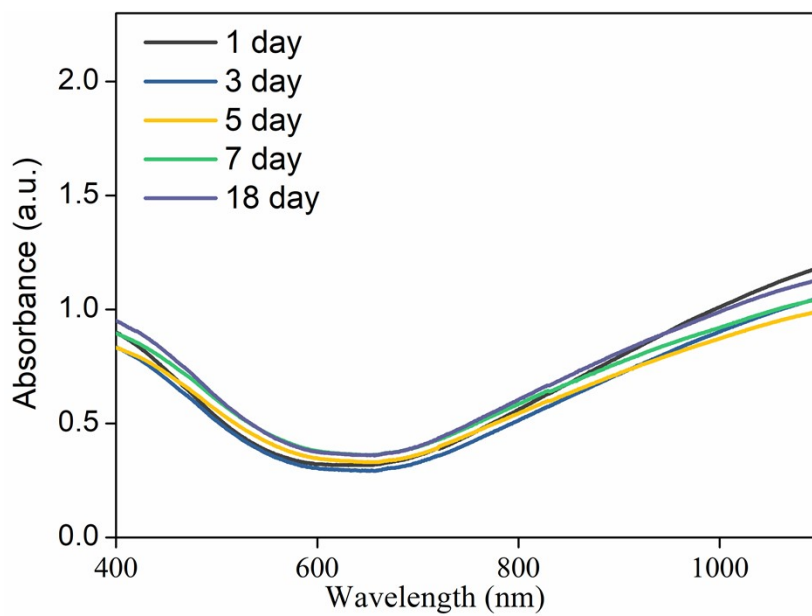


Figure S7. The UV-vis-NIR absorption spectra of Cys-CuS nanosheets (50 mg L^{-1}) solutions after store for different durations.

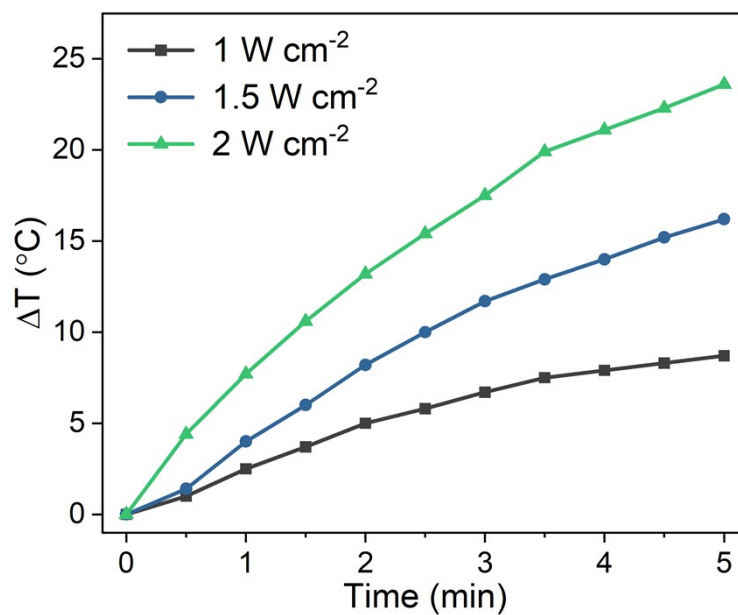


Figure S8. Temperature curves Cys-CuS nanosheets (200 mg L⁻¹) solutions upon irradiation of 1064 nm laser (1, 1.5, 2.0 W cm⁻², 5 min).

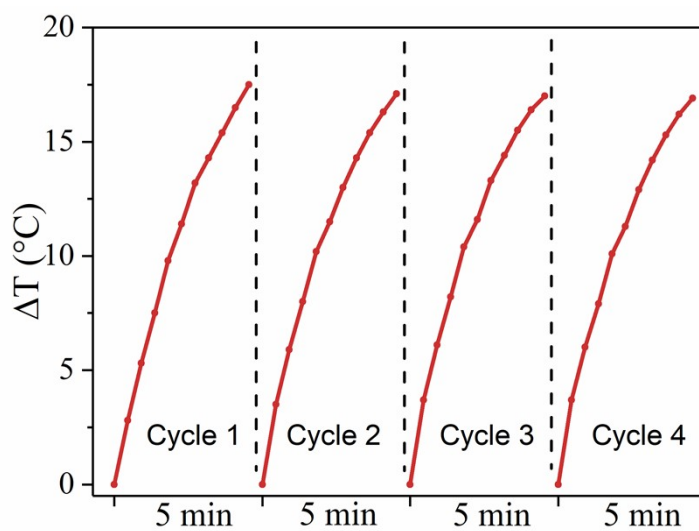


Figure S9. Photothermal stability of Cys-CuS nanosheets (100 mg L⁻¹) under cyclic irradiation of 1064 nm laser (2 W cm⁻²).

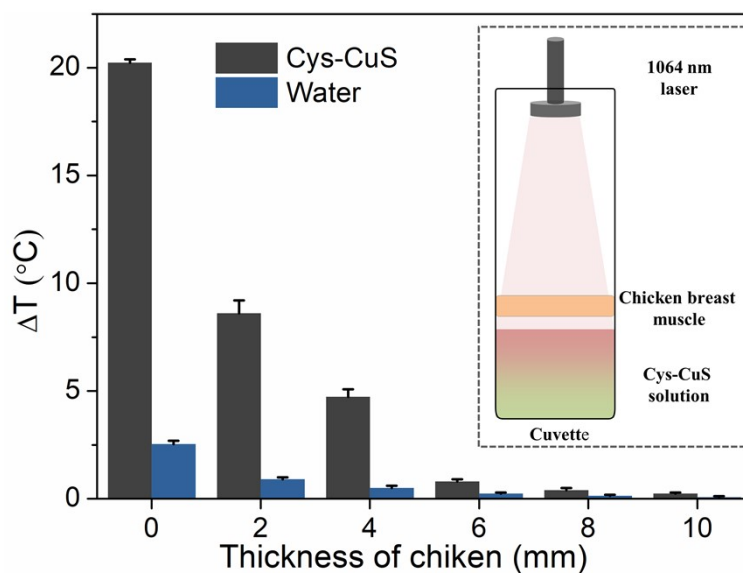


Figure S10. Deep-tissue photothermal study of Cys-CuS nanosheets (80 mg L^{-1} , 1 mL) covered by different thicknesses of chicken breast muscle (2, 4, 6, 8, 10 mm) under a 1064 nm laser irradiation (1 W cm^{-2} , 2 min).

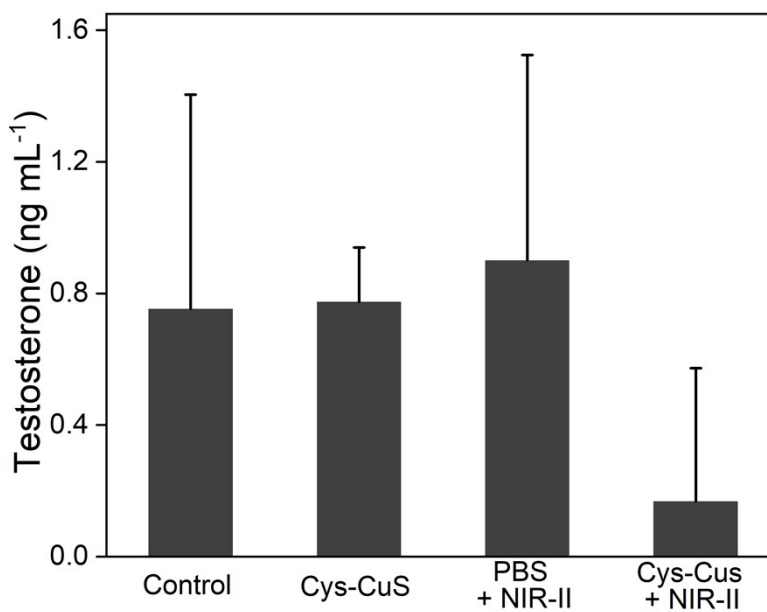


Figure S11. Plasma levels of testosterone in mice at 60th day post treatments.

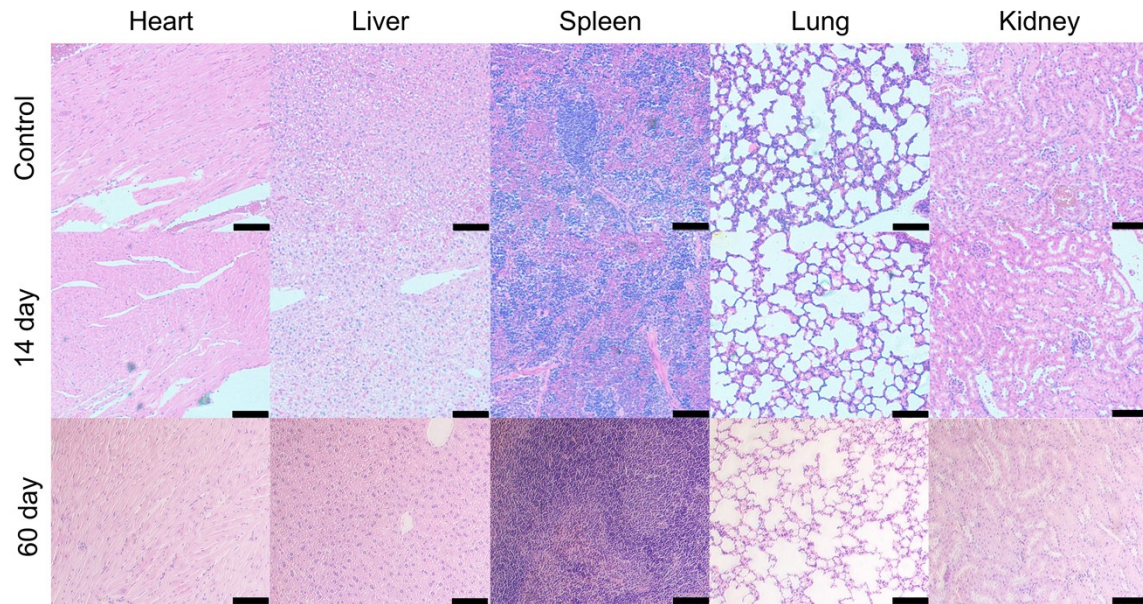


Figure S12. H&E staining of major organs from mice after intra-testicular injection with or without Cys-CuS nanosheets (100 μL , 100 mg L^{-1}). (Scale bar: 100 μm)